

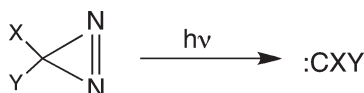
“Carbon Dichloride”: Dihalocarbenes Sixty Years After Hine^{1,2}

Robert A. Moss*

Wright and Rieman Laboratories, Department of Chemistry and Chemical Biology, Rutgers,
The State University of New Jersey, New Brunswick, New Jersey 08903

moss@rutchem.rutgers.edu

Received March 2, 2010

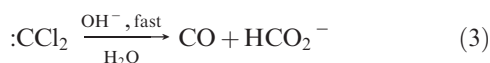
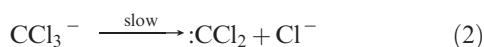
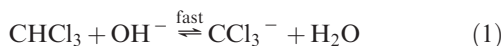


We describe new syntheses of dichlorodiazirine, difluorodiazirine, and chlorofluorodiazirine. From these precursors, laser flash photolysis enables the generation of CCl_2 , CF_2 , and CClF . We describe the formation and chemistry of bromodichloromethide carbanion from CCl_2 , the ambiplicity of CCl_2 , the complexation of CCl_2 by aromatic ethers, and the kinetics and activation parameters attending the additions of CCl_2 , CF_2 , and CClF to several alkenes.

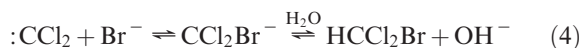
Introduction

In his seminal 1960 report on the mechanism of the basic hydrolysis of chloroform,³ Jack Hine noted that the proposed intermediacy of “carbon dichloride” (i.e., dichlorocarbene, CCl_2)⁴ was an old idea. Already in 1862, Geuther had proposed that the basic hydrolysis of chloroform to carbon monoxide and formate ion involved CCl_2 .⁵ In Geuther’s formulation, “chloroform” is actually $\text{CCl}_2 \cdot \text{HCl}$ and “the hydrogen chloride may be removed by alkalai to give carbon dichloride, which is further hydrolyzed to carbon monoxide.”³ Similar ideas were offered by Nef,⁶ Thiele,⁷ and Mossler⁸ from 1897 to 1903.

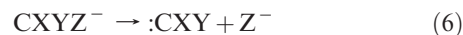
It remained, however, for Hine to establish the intermediacy of CCl_2 by kinetics and mechanistic studies nearly 90 years after Geuther’s suggestion.^{3,9} Hine’s mechanism is shown in eqs 1–3 and features the rapid, reversible formation of the trichloromethide carbanion (CCl_3^-) followed by its rate-determining scission into CCl_2 and chloride ion.



Hine demonstrated that CCl_2 could be captured by sodium thiophenylate, ultimately giving phenyl orthothioformate,³ and also by bromide or iodide ions, leading to the CCl_2Br^- or CCl_2I^- trihalomethide carbanions which yielded the corresponding haloforms on protonation;¹⁰ e.g., eq 4.

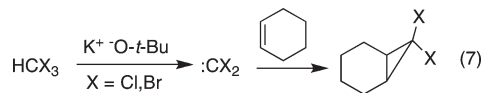


Generalizing the reverse reaction, Hine showed that a variety of trihalomethide carbanions, CXYZ^- , was available by the deprotonation of haloforms, thus making accessible an entire family of dihalocarbenes;¹¹ cf. eqs 5 and 6.



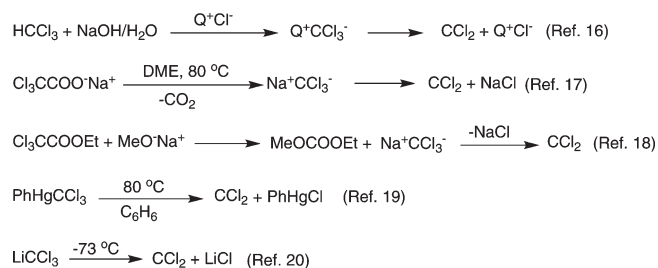
The haloforms included CHI_3 , CHBr_3 , CHBr_2Cl , CHCl_2F , CHBrCl_2 , and CHBrClF . However, with difluorohaloforms (CHXF_2), Hine found that the trihalomethide anion (CXF_2^-) was bypassed; the haloform reacted with base in a concerted fashion, eliminating HX and directly affording the highly stabilized difluorocarbene.¹²

Building on Hine’s pioneering research, Doering and Hoffmann found that CCl_2 or CBr_2 , generated by the basic decomposition of chloroform or bromoform, could be captured by olefins (e.g., cyclohexene), affording the corresponding cyclopropanes; eq 7.¹³ This was the first of hundreds of related dihalocyclopropanations which have become enormously important in synthetic and mechanistic organic chemistry.¹⁴

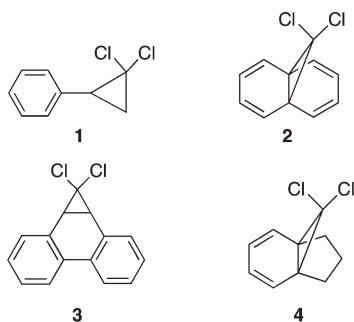


There are many other methods for the generation of CCl_2 (and other dihalocarbenes) that proceed via trihalomethide carbanions or involve organometallic precursors;¹⁵ some of these are illustrated in Chart 1.^{16–20}

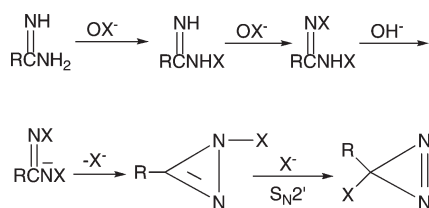
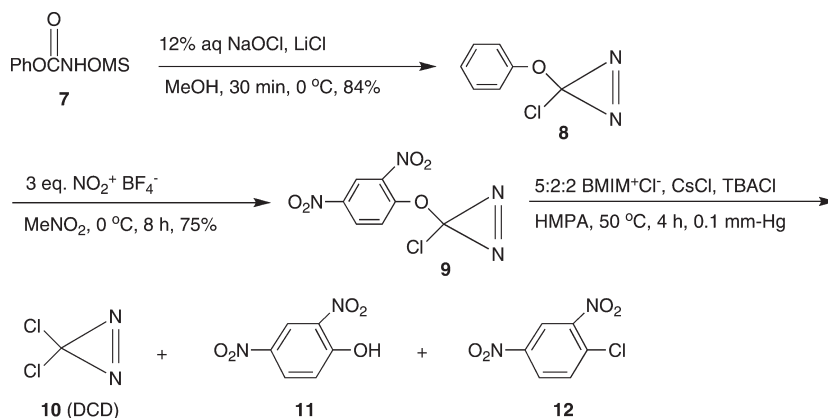
However, these methods do not allow the *spectroscopic* study of CCl_2 chemistry. In order to study certain fundamental reactions of CCl_2 , or CX_2 in general, we require clean

CHART 1. Some Methods for the Generation of Dichlorocarbene


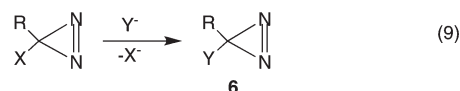
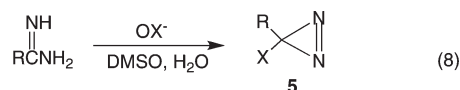
photochemical sources of the carbenes. Photochemical precursors of CCl_2 are known, for example, the CCl_2 adducts of styrene (**1**),²¹ naphthalene (**2**),²² phenanthrene (**3**),²³ and indan (**4**).²⁴ CCl_2 can be liberated from **1–4** by photoextrusion, but the accompanying aromatic byproducts can complicate spectroscopic analysis. Thus, CCl_2 could not be visualized following its laser flash photolytic (LFP) generation from adduct **3** due to interference from absorptions of triplet phenanthrene.



Our approach to this problem envisioned the synthesis of *dihalodiazirines* from which the dihalocarbenes could be

SCHEME 1. Mechanism of the Graham Reaction

SCHEME 2. Synthesis of Dichlorodiazirine


photochemically generated, accompanied by the “user-friendly” nitrogen leaving group. Our strategy combined two methods of diazine synthesis: the Graham reaction,²⁵ eq 8, and the diazine exchange reaction,²⁶ eq 9. In the Graham reaction an amidine ($\text{R} = \text{alkyl, alkoxy, aryl, aryloxy, or vinyl}$) is oxidized with aqueous hypohalite (OCl^- or OBr^-) to the corresponding halodiazirine **5**. The mechanism of this remarkable one-pot reaction is complicated, but its scope is wide and many examples are known. A plausible mechanism is shown in Scheme 1.²⁷ Here, successive *N*-halogenations convert the amidine to a *N,N'*-dihaloamidine which is then deprotonated to the *N*-anion, the latter closes to a *N*-haloisodiazirine (possibly via a nitrene), which is finally converted to the desired halodiazirine by a $\text{S}_{\text{N}}2'$ reaction with halide ion.

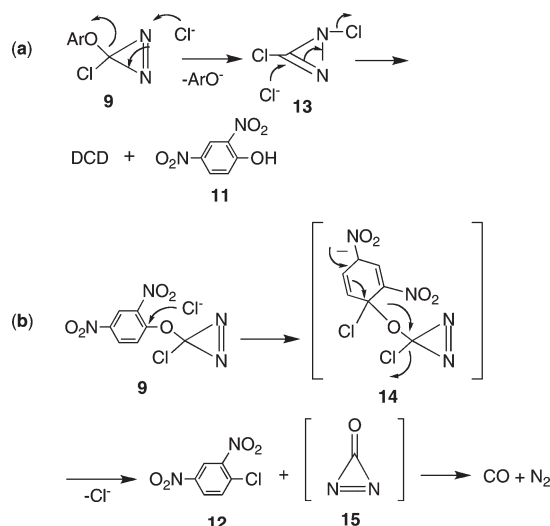


Importantly, the halide ($\text{X} = \text{Cl, Br}$) of halodiazirine **5**, can be readily *exchanged* for other nucleophiles (Y), as shown in eq 9.^{26,28} One can thus introduce F, CN, MeO, PhO, AcO, or ArO groups as “Y” into diazine **6**. Together, eqs 8 and 9 provide a basis for the preparations of dichlorodiazirine and its close relatives.

Syntheses of Three Dihalodiazirines

Our synthesis of dichlorodiazirine is outlined in Scheme 2.^{29,30} The initial step is a Graham oxidation in which the mesylate derivative of phenyl isourea **7**³¹ is converted to phenoxychlorodiazirine **8**.³² The second step, dinitration of the *O*-activated phenyl group of **8** with nitronium tetrafluoroborate, affords 2,4-dinitrophenoxychlorodiazirine **9**, in which the phenoxy moiety of **8** is transformed into a 2,4-dinitrophenoxy *leaving group*, suitable for the diazine exchange reaction, cf. eq 9.³³ Indeed, reaction of **9** with a nucleophilic chloride blend of tetrabutylammonium (TBA) chloride, cesium chloride, and butylmethylimidazolium chloride in a minimum volume of HMPA at 50°C for 4 h gave dichlorodiazirine

SCHEME 3. Diazirine Partition Mechanism



(10, DCD), which was removed under vacuum and trapped in pentane at 77 K.³⁰

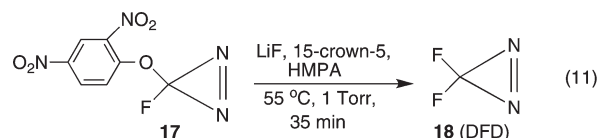
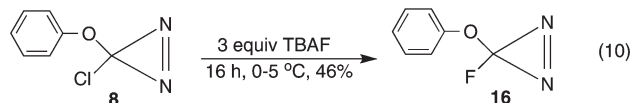
The UV spectrum of DCD in pentane reveals a number of bands in the 327–359 nm region, so that DCD is well-suited for LFP experiments using our xenon fluoride excimer laser with emission at 351 nm. DCD also displays an IR band at 1548 cm⁻¹ which can be assigned to its N=N stretch. Pentane solutions of DCD are moderately stable in the dark; about 10% decomposition occurs over 13 h.²⁹ The activation energy for cleavage of DCD to CCl₂ and N₂ is computed at 28 kcal/mol [B3LYP/6-311+G(2d,p)].

Accompanying the production of DCD (Scheme 2), we also find two high-boiling products: 2,4-dinitrophenol (**11**, 20%) and 2,4-dinitrochlorobenzene (**12**, 80%). Their formation can be understood in terms of the partition mechanism depicted in Scheme 3.^{29,30} Partition branch (a) is the “normal” diazirine exchange reaction, in which chloride attacks diazirine **9** at N, displacing 2,4-dinitrophenoxide in a S_N2' fashion, while generating intermediate dichloroisodiazirine **13**. The latter is then converted to DCD by a second S_N2' reaction with chloride, while protonation of the 2,4-dinitrophenoxide expelled in the preceding step affords 2,4-dinitrophenol **11**.

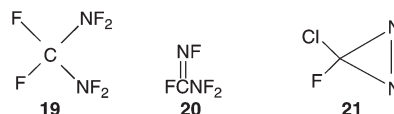
Simultaneously, and competitively, chloride also attacks substrate **9** at C(1) of its activated 2,4-dinitrophenyl moiety; cf. branch (b) of Scheme 3. Decomposition of the resulting Meisenheimer complex (**14**) affords 2,4-dinitrochlorobenzene **12** and (nominally) diazirinone **15**.³⁴ Diazirinone is unstable, however, and should decompose to carbon monoxide and nitrogen. Our assignment of a transient IR band at 2150 cm⁻¹ (observed in the reaction of *p*-nitrophenoxychlorodiazirine with fluoride) to diazirinone, is probably incorrect.³⁵ The 2150 cm⁻¹ band more likely represents CO in the condensed phase which subsequently resolves into two bands at 2116 and 2173 cm⁻¹ as the CO enters the gas phase.³⁵

Products **11** and **12** are obtained in a 1:4 distribution, indicating that the partition in Scheme 3 favors (unproductive) branch (b) over DCD-yielding branch (a). Nevertheless, the reaction sequence of Scheme 2 represents the first preparation of DCD and enables some previously impossible studies of the chemistry of CCl₂.^{2,30}

The methodology described in Scheme 2 can be easily extended to syntheses of difluorodiazirine³⁶ and chlorofluorodiazirine.³⁷ The key interpolation in the former case is the conversion of phenoxychlorodiazirine **8** to phenoxyfluorodiazirine **16** by diazirine exchange with fluoride ion; eq 10.³⁸ Nitration of **16** with NO₂⁺BF₄⁻ then gives 2,4-dinitrophenoxylfluorodiazirine (**17**) in 78% yield, and the latter affords difluorodiazirine (**18**, DFD) upon reaction with LiF and 15-crown-5 in HMPA at 55 °C; cf. eq 11. The reaction of **17** with fluoride is subject to a partition analogous to that of Scheme 3, but here branch (a) is favored over branch (b) by 3:1, so that the formation of DFD is accompanied by 2,4-dinitrophenol and 2,4-dinitrofluorobenzene in a 3:1 distribution.



The UV spectrum of DFD in pentane exhibits maxima at 324, 334, 339, 351, and 356 nm, very similar to the UV spectrum of DCD, and in general agreement with the published gas-phase spectrum of DFD.³⁹ Indeed, DFD was previously prepared by the ferrocene reductive defluorination of bis(difluoroamino)difluoromethane (**19**) or tetrafluoroformamidine (**20**), but these precursors are explosive and inconvenient.⁴⁰ DFD is also available by the CsF-mediated rearrangement of difluorocyanamide (F₂NCN), but this precursor too is “highly explosive.”⁴¹



In analogy to eq 11, treatment of **17** with TBACl in HMPA at ambient temperature produces chlorofluorodiazirine **21**, which is removed under vacuum as it forms and trapped in pentane. Its UV spectrum displays multiple absorptions between 320 and 356 nm, in excellent agreement with the published (gas phase) spectrum for **21** previously prepared by the reductive-defluorination of an explosive trifluoroamidine precursor.^{39c,42} Our initial synthesis of **21** involved the reaction of *p*-nitrophenoxychlorodiazirine with fluoride, but the alternative reaction of **17** with chloride is more efficient.

The syntheses of DCD, DFD, and chlorofluorodiazirine described here allow us to perform various spectroscopy-based experiments with CCl₂, CF₂, and CClF that were hitherto impossible. Some examples are described in succeeding sections of this Perspective.

Trihalomethide Carbanions

LFP of DCD generates CCl₂ which is readily intercepted by, e.g., pyridine or thioanisole to yield the

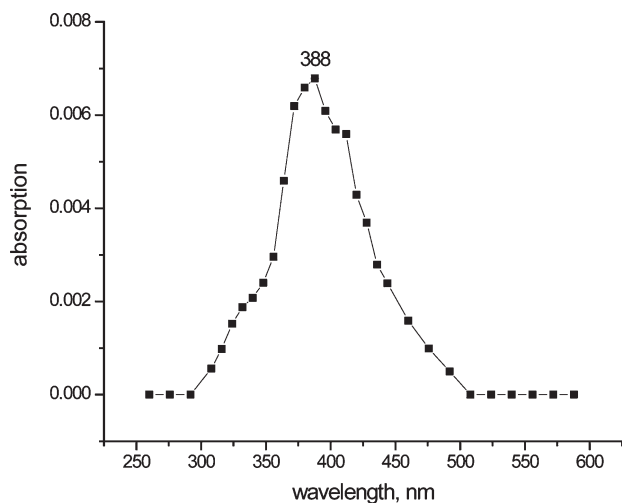
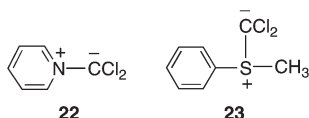
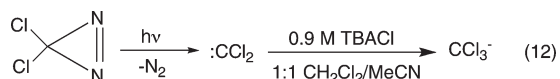


FIGURE 1. UV-vis spectrum acquired 50 ns after LFP of dichlorodiazirine with 0.6 M TBABr in 1:1 CH_2Cl_2 -MeCN under nitrogen; the absorption of CCl_2Br^- is at 388 nm. Reprinted from ref 43 with permission of the American Chemical Society.

UV-active ylides **22** (λ_{max} 387 nm) or **23** (λ_{max} 432 nm), respectively.



Our ability to photochemically generate CCl_2 from DCD permits us to conveniently study the *reverse* of Hine's classic reaction, eq 2; i.e., the addition of chloride or other halides to CCl_2 with the formation of trihalomethide carbanions. LFP of DCD in the presence of chloride ions affords the trichloromethide carbanion (CCl_3^-), visible as a weakly absorbing species at 328 nm; cf. eq 12.⁴³



Calculations at the TD B3LYP/6-311+G(d)//PBE/6-311+G(d) level of theory (in CPCM simulated MeCN) predict the absorbance of CCl_3^- at 344 nm and suggest that the conversion of CCl_2 to CCl_3^- is exothermic ($\Delta H = -8.4$ kcal/mol, $\Delta G = -3.0$ kcal/mol).

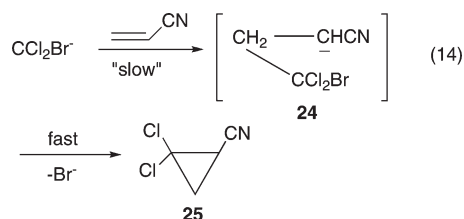
An analogous reaction of CCl_2 with bromide affords the more strongly absorbing bromodichloromethide carbanion (CCl_2Br^-), cf. eq 13 and Figure 1. The dominant absorption at 388 nm is assigned to CCl_2Br^- , computed to absorb at 376 nm in MeCN. The shoulder visible at 404 nm is assigned to CClBr_2^- (predicted at 401 nm), which could be formed from CCl_2Br^- by exchange with Br^- via the carbene, CClBr . Both CCl_2Br^- and CClBr_2^- are persistent species with lifetimes in excess of 1500 ns. The shoulder at 330 nm in Figure 1 *might* be due to CCl_3^- , possibly obtained by reaction of CCl_2 with Cl^- released from CCl_2Br^- during the latter's conversion to CClBr_2^- . However, the transient at 330 nm is unstable and decays after 200 ns.



The formation of CCl_2Br^- from CCl_2 and Br^- is computed to be thermodynamically favorable ($\Delta H = -7.7$ kcal/mol; $\Delta G = -2.5$ kcal/mol). However, the conversion of CCl_2Br^- to CClBr_2^- appears to be slightly unfavorable with $\Delta H = 0.6$ kcal/mol and $\Delta G = 0.5$ kcal/mol.

The chemistry of CCl_2Br^- can be easily examined by LFP. For example, its rate of formation via eq 13 can be measured as $2.08 \times 10^7 \text{ M}^{-1} \text{ s}^{-1}$ from the slope of a correlation of the observed rate constants for the rise of CCl_2Br^- at 380 nm versus the concentration of Br^- .

Next, we studied the Michael addition of CCl_2Br^- to acrylonitrile as shown in eq 14. This reaction most likely proceeds via rate-determining formation of intermediate carbanion **24**, which rapidly closes to the product, 1,1-dichloro-2-cyanocyclopropane (**25**), with loss of bromide. A correlation of k_{obs} for the decay of the CCl_2Br^- absorbance at 380 nm versus the concentration of acrylonitrile (in the presence of 0.72 M TBABr) gives $k = 4.07 \times 10^6 \text{ M}^{-1} \text{ s}^{-1}$ for the first step of eq 14.



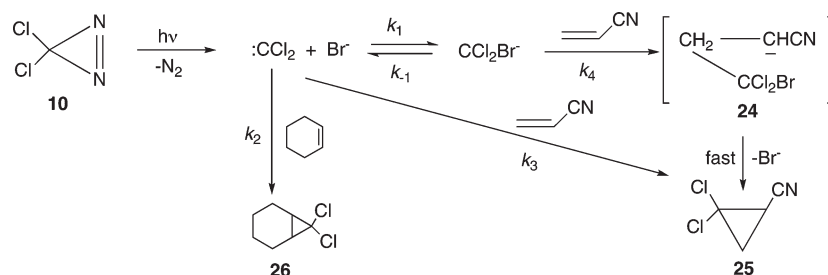
Equation 14 also represents *bromide ion catalysis* of the addition of CCl_2 to acrylonitrile. CCl_2 usually behaves as an *electrophile* in addition to alkenes⁴⁴ (see, however, below). Its *direct* addition to electron-poor acrylonitrile occurs with $k = 4.9 \times 10^5 \text{ M}^{-1} \text{ s}^{-1}$,⁴⁵ so that the bromide-assisted Michael addition of eq 14, where $k = 4.07 \times 10^6 \text{ M}^{-1} \text{ s}^{-1}$, represents a rate increase of 8.3. This catalytic process is rather general; analogous results were obtained in the bromide-assisted additions of phenylhalocarbenes to acrylonitrile, where rate accelerations of 14–28 were recorded relative to the direct carbene additions.⁴⁶

Another way to assess bromide assistance considers the relative rate constant (k_{rel}) for the competitive addition of CCl_2 to electron-poor acrylonitrile vs the more nucleophilic cyclohexene. We find that k_{rel} increases from 0.0077 in the direct addition of CCl_2 to 0.18 in the presence of 0.28 M Br^- , representing a 23-fold enhancement in the apparent reactivity of acrylonitrile due to the bromide-assisted addition described in eq 14.

Scheme 4 depicts competing unassisted and assisted pathways in the additions of CCl_2 to acrylonitrile and cyclohexene. Here, CCl_2 generated by LFP of DCD (**10**) either reacts with Br^- to give CCl_2Br^- ($k_1 = 2.1 \times 10^7 \text{ M}^{-1} \text{ s}^{-1}$), adds to cyclohexene to yield dichloronorcaradiene **26** ($k_2 = 6.4 \times 10^7 \text{ M}^{-1} \text{ s}^{-1}$), or adds directly to acrylonitrile affording product **25** ($k_3 = 4.9 \times 10^5 \text{ M}^{-1} \text{ s}^{-1}$). Carbanion CCl_2Br^- can either revert to CCl_2 and Br^- (k_{-1}) or add to acrylonitrile to give carbanion **24** ($k_4 = 4.1 \times 10^6 \text{ M}^{-1} \text{ s}^{-1}$), which rapidly closes to cyclopropane **25**.

With these rate constants, and our observation that the apparent value of $k_3/k_2 = 0.18$ in the presence of 0.28 M Br^- , we can estimate that the equilibrium constant (K), which governs the interconversion of CCl_2 and CCl_2Br^- , is $\sim 10 \text{ M}^{-1}$ in Scheme 4. Given that $K = k_1/k_{-1}$, we can extract

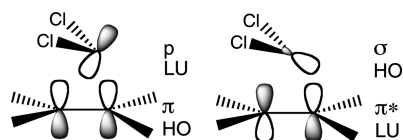
SCHEME 4. Reactions of Dichlorocarbene and Bromodichloromethide Carbanion

TABLE 1. Relative Reactivities of CCl_2 toward Alkenes^a

alkene	substitution	k_{rel}
$\text{Me}_2\text{C}=\text{CMe}_2$	tetra	53.7
$\text{Me}_2\text{C}=\text{CHMe}$	tri	23.5
$\text{Me}_2\text{C}=\text{CH}_2$	di	8.32
cyclohexene	di	1.00
$n\text{-PrCH}=\text{CH}_2$	mono	0.14

^aData from ref 48.TABLE 2. Absolute Rate Constants and Activation Energies for CCl_2 -Alkene Additions^{a,b}

alkene	$k_{\text{CCl}_2} (\text{M}^{-1} \text{s}^{-1})$	E_a (kcal/mol)
$\text{Me}_2\text{C}=\text{CMe}_2$	4.7×10^9	
$\text{Me}_2\text{C}=\text{CHMe}$	2.5×10^9	
cyclohexene	6.4×10^7	3.8
$n\text{-BuCH}=\text{CH}_2$	1.8×10^7	4.7
$\text{CH}_2=\text{CHCOOMe}$	5.9×10^5	6.7
$\text{CH}_2=\text{CHCN}$	4.9×10^5	6.9
$\text{CH}_2=\text{CClCN}$	8.1×10^6	5.4

^aData from refs 37, 45, and 53. ^bIn pentane at 24 °C.FIGURE 2. HOMO-LUMO interactions in CCl_2 /alkene cycloadditions. Reprinted from ref 45 with permission of the American Chemical Society.

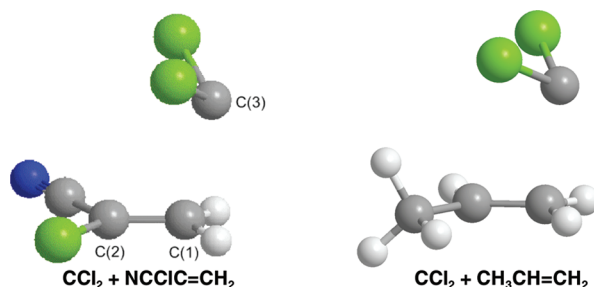
$k_{-1} \sim 2.1 \times 10^6 \text{ s}^{-1}$ for the reversion of CCl_2Br^- to CCl_2 and Br^- .^{43,47}

The Philicity of Dichlorocarbene

On the basis of relative reactivity studies, Doering concluded in 1958 that CCl_2 was an electrophile.⁴⁸ The data, shown in Table 1, indicate that CCl_2 is more reactive toward more highly alkylated, more electron-rich, more nucleophilic alkenes. Dibromocarbene exhibits a similar reactivity pattern, as demonstrated by Skell in 1956.⁴⁹

More generally, any singlet carbene is inherently *both* an electrophile and a nucleophile. In terms of frontier molecular orbital theory, philicity depends on whether the “electrophilic” carbene-LUMO (p)/alkene-HOMO (π) or the “nucleophilic” carbene-HOMO (σ)/alkene-LUMO (π^*) orbital interaction dominates in the cycloaddition transition state and governs the direction of charge transfer between the carbene and the alkene; cf. Figure 2.^{44,45,50–52} If the carbene p/alkene π interaction dominates, the carbene will exhibit *electrophilic* behavior; if the carbene σ /alkene π^* interaction is dominant, *nucleophilic* discrimination will be displayed. If both interactions are comparable, the carbene will manifest an *ambiphilic* selectivity pattern, acting as an electrophile toward electron-rich alkenes, but as a nucleophile toward electron-poor alkenes.^{44,51,52}

Due to its very low-lying LUMO,^{44,51} CCl_2 almost always reacts with alkenes via a dominant carbene p/alkene π (i.e., electrophilic) interaction. The absolute rate constants and activation energies collected in Table 2^{37,45,53} illustrate this behavior for a series of electron-rich alkenes through the electron-poor alkenes, methyl acrylate and acrylonitrile: rate

FIGURE 3. Computed transition states for additions of CCl_2 to α -chloroacrylonitrile (left) and to propene (right). Reprinted from ref 45 with permission of the American Chemical Society.

constants decrease and activation energies increase as electron-donating alkyl groups are removed and electron-withdrawing substituents are imposed on the alkenes.

However, if the alkene is made excessively electron-poor, so that its LUMO or π^* orbital is sufficiently lowered, then CCl_2 can react as a nucleophile via its σ electron pair. This is seen with α -chloroacrylonitrile (Table 2) where, compared to acrylonitrile, the rate of CCl_2 addition *increases* and the activation energy *decreases*.

Computational studies at the B3LYP/6-311+G(d) level support the nucleophilic character of the CCl_2 /chloroacrylonitrile addition transition state. Figure 3 depicts the computed transition states for additions of CCl_2 to chloroacrylonitrile and propene, where the latter addition is electrophilic. In particular, charge transfer in the CCl_2 /propene transition state is 0.07e from alkene to carbene, whereas it is 0.06e in the *opposite direction* (carbene to alkene) in the CCl_2 /chloroacrylonitrile transition state.

Another philicity indicator is the carbene tilt angle, defined as the angle between the bisector of the carbene's Cl-C-Cl angle and the alkene's carbon-carbon double bond at the transition state. For a purely electrophilic, solely p-orbital carbene attack, the tilt angle would be 0°. For a purely nucleophilic, solely σ -orbital carbene attack, the tilt angle would be 90°. Tilt angles larger than 45° signal

substantial nucleophilic character in a carbene addition, whereas tilt angles less than 45° are consistent with predominant electrophilic character. The CCl_2 -propene transition state (Figure 3) exhibits a tilt angle of 42° and can be classified as electrophilic. However, the tilt angle of the CCl_2 -chloroacrylonitrile transition state is 49.6° , indicative of nucleophilic character.

The moral of this story is that CCl_2 , and other commonly “electrophilic” carbenes, can behave as nucleophiles when presented with appropriately electron-deficient substrates. In other words, almost all singlet carbenes are least potentially *ambiphilic*.

Solvation and Complexation of Dichlorocarbene

In 2007, we reported that the weak $\sigma \rightarrow \text{p}$ electronic transitions of methylchlorocarbene and benzylchlorocarbene could be detected by LFP with UV-vis detection in solution at ambient temperatures.⁵⁴ Moreover, these absorptions could be used to directly monitor carbene-solvent interactions. In particular, theoretical predictions of, e.g., methylchlorocarbene-anisole complex formation⁵⁵ could be demonstrated by observational studies.

Very recently, we found that CCl_2 formed analogous π and ylidic complexes with a variety of aromatic ethers.⁵⁶ Although the computed $\sigma \rightarrow \text{p}$ absorbance of CCl_2 at 492 nm in pentane could not be observed in our solution experiments, LFP of DCD in a 1:1 anisole-pentane solution afforded weak absorptions at 460 and 500 nm (Figure 4) which we assigned to ylidic and π complexes of CCl_2 with anisole.^{56,57} The complexes formed with $k_f = 1.6 \times 10^7 \text{ s}^{-1}$ (460 nm) and $k_f = 6.4 \times 10^6 \text{ s}^{-1}$ (500 nm), indicating that the complexation was fast, but not diffusion-controlled. There appeared to be a barrier to complexation.⁵⁸ Decay of the complexes was also rapid, with $k_d = 3.1 \times 10^5 \text{ s}^{-1}$ (460 nm) and $1.5 \times 10^6 \text{ s}^{-1}$ (500 nm).

Structures, complexation energies [PBE/6-311+G(d)], and electronic transitions [B3LYP/6-311+G(d) with CPCM solvent corrections] were computed for the CCl_2 -anisole complexes, and two of the several located complexes are shown in Figure 5. The *O*-ylidic complex ($\text{C}-\text{O} = 2.6 \text{ \AA}$) is computed to exhibit a (*O*) $\text{n} \rightarrow \text{p}$ (carbene) absorption at 486 nm ($f = 0.11$), which we assign to the observed band at 460 nm (Figure 4), while the (para) π -complex ($\text{C}-\text{C} = 2.8 \text{ \AA}$) is computed to display a (phenyl) $\pi \rightarrow \text{p}$ (carbene) absorption at 513 nm ($f = 0.15$), which we assign to the signal observed at 500 nm.

The formation of these complexes is computed to be enthalpically favorable ($\Delta H = -2.7$ and -2.5 kcal/mol , respectively), although the free energies of formation are unfavorable ($\Delta G = 3.7$ and 4.6 kcal/mol , respectively). With $\Delta G > 0$, the concentration of the complexes will be low. However, there will be many geometrically similar complexes of comparable energy, so that the absorbance of the complexes will be detectable, if still weak.

In addition to anisole (**27**), analogous π and *O*-ylidic complexes of CCl_2 were observed for a number of aryl ethers (**28–31**), and for the aryl ester, phenyl acetate (**32**). However, we did not observe CCl_2 complexes of simple ethers such as THF, dioxane, or 18-crown-6. Computationally, the enthalpies and free energies of formation of the CCl_2 /THF and CCl_2 /dioxane complexes were considerably less favorable

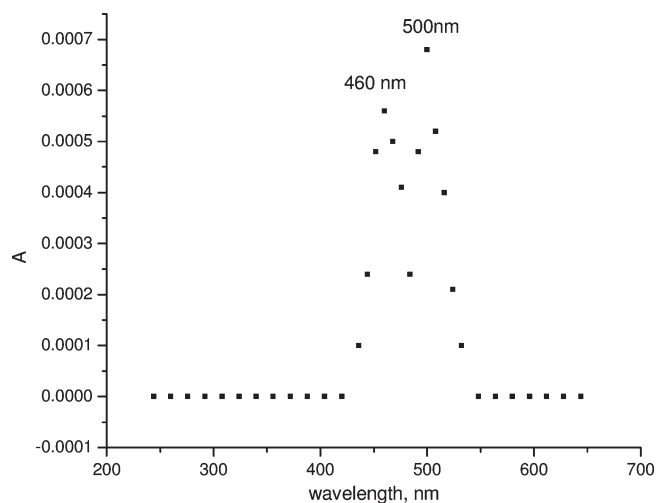


FIGURE 4. LFP UV spectrum of CCl_2 in 1:1 anisole-pentane solution 150 ns after the laser pulse; complexes at 460 and 500 nm. Reprinted with from ref 56 with permission of the American Chemical Society.

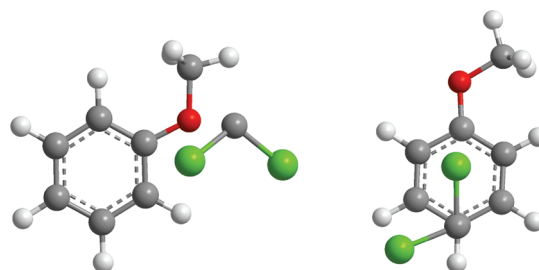
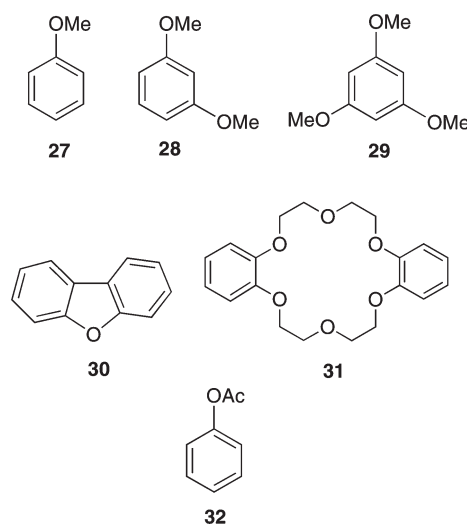


FIGURE 5. Computed *O*-ylidic complex (left) and π -complex (right) of CCl_2 and anisole. Reprinted from ref 56 with permission of the American Chemical Society.

than those of CCl_2 with substrates **27–32**. Previous studies also suggested little effect of THF or dioxane on the properties of CCl_2 .²⁴



Computational studies also predicted complexation between CCl_2 and methyl-substituted benzenes like mesitylene (**33**) and durene (**34**), but the anticipated absorptions in the 340–360 nm spectral region were not observed.

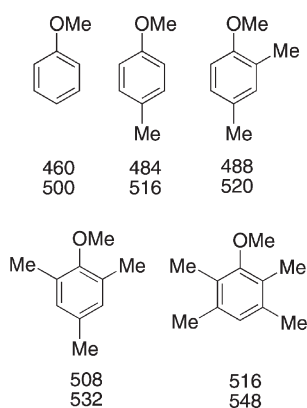
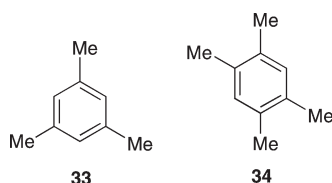


FIGURE 6. CCl_2 complex formation with methylanisoles. The wavelengths of the complex's absorptions (nm) are shown beneath the structure of each methylanisole.

The sensitivity of our LFP–UV detection system might be low in this spectral region because of strong background absorption by DCD (λ_{max} 324, 359 nm in pentane).



We reasoned that substitution of a methoxy group for a proton on **33** or **34** would shift the absorbances of the corresponding CCl_2 complexes toward the red and into the 400–500 nm region where they might be more easily seen. This proved to be a fruitful idea.⁵⁹ Figure 6 depicts four incrementally methyl-substituted derivatives of anisole. Each forms observable complexes with CCl_2 , and each additional methyl substituent induces a red shift in each absorbance, behavior that is consistent with $\sigma \rightarrow \text{p}$ or $\pi \rightarrow \text{p}$ origins for the absorbances. O or π electronic transitions from the anisole to the vacant carbenic p orbital are assisted by increasing the number of donor methyl groups on the anisole.

Figure 7 presents one of several complexes computed for CCl_2 and 2,4,6-trimethylanisole at the B3LYP/6-311+G(d)//PBE/6-311+G(d) level of theory. This C(1) π -complex is computed to have $\Delta H = -3.0$ kcal/mol, $\Delta G = 3.8$ kcal/mol, and C–C = 2.9 Å. It is predicted to absorb at ~ 490 nm ($f \sim 0.1$), which can be correlated with the observed absorbance at 508 nm.⁶⁰

Red shifts of anisole– CCl_2 complex absorptions are also induced by additional methoxy substituents. The 460 and 500 nm absorptions (Figure 4) of the CCl_2 –anisole complexes (CCl_2 –**27**, cf. Figure 5) shift to 500 and 548 nm for the CCl_2 –**28** complexes and to 580 and 660 nm for the CCl_2 –**29** complexes. Indeed, the π -complexes of CCl_2 with **29** (Figure 8) are computed to be the most stable that we have encountered, with $\Delta H \approx -9$ kcal/mol and $\Delta G \approx 2$ kcal/mol. Their anticipated absorbances are shifted far into the visible at 607 and 683 nm, in reasonable accord with the observed signals at 580 and 660 nm.

The CCl_2 –**29** π -complexes in Figure 8 reflect the substantial electron density at C(2) of substrate **29**. Indeed, an O -ylidic complex of **29** is computed to be both

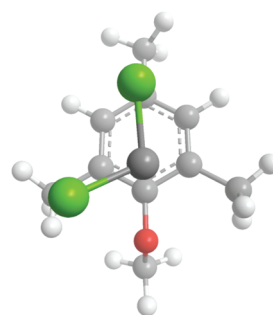


FIGURE 7. Computed structure of CCl_2 complex with 2,4,6-trimethylanisole. Reprinted with permission from ref 59.

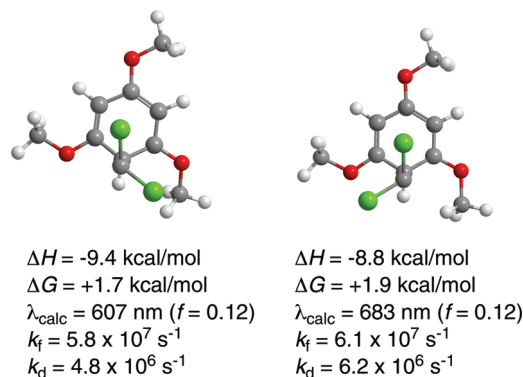


FIGURE 8. Computed structures for π -complexes of CCl_2 with 2,4,6-trimethoxyanisole. Reprinted from ref 56 with permission of the American Chemical Society.

thermodynamically and kinetically unfavorable, relative to the π -complexes. The latter should readily decay to a dichloronorcaradiene product over very low barriers ($\Delta G^\ddagger \sim 2$ kcal/mol) which presumably arise from the loss of aromaticity accompanying the cyclopropanation. Indeed, k_d for the π -complexes is $(5\text{--}6) \times 10^6$ s⁻¹, although the product of decay has not yet been studied.

Starting from separated CCl_2 and **29** we calculate no potential energy barriers to the formation of the CCl_2 –**29** complexes. Nevertheless, the LFP experimental rate constants for their formation are only $(5\text{--}6) \times 10^7$ s⁻¹, about 2 orders of magnitude less than diffusion control. What accounts for this discrepancy?

We measured k_f between 283 and 308 K for the formation of the CCl_2 –**29** π -complex absorbing at 580 nm (Figure 8, left-hand structure). An Arrhenius correlation of the data gave $E_a = -1.8$ kcal/mol and $\Delta H^\ddagger = -2.4$ kcal/mol, confirming the absence of a potential energy barrier to complex formation. The negative E_a is preceded in the similarly negative activation energies observed for the additions of CCl_2 and PhCCl_2 ⁶¹ to the highly reactive alkene, tetramethylethylene.

Moreover, the Arrhenius results afford $\log A = 6.81$ s⁻¹ and $\Delta S^\ddagger = -29$ eu for complexation of CCl_2 and **29**, leading to $\Delta G^\ddagger = 6.4$ kcal/mol. There is thus a free energy barrier to the complexation arising from the very unfavorable ΔS^\ddagger , presumably a consequence of unfavorable translational, vibrational, rotational, and solvent reorganization effects as the two reactants combine to give a single product. This rationalizes the slower than diffusion-controlled complexation kinetics. Indeed, Houk and Rondan demonstrated that

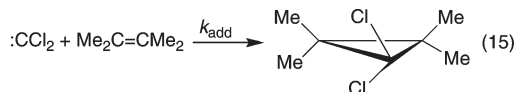
TABLE 3. Rate Constants for Additions of CCl₂ to TME^a

solvent or additive	k_{add} (M ⁻¹ s ⁻¹)	$k_{\text{pent}}/k_{\text{add}}$
pentane ^b	4.7×10^9	1.0
mesitylene ^c	3.2×10^8	15
anisole ^c	2.6×10^8	18
TMA ^d	4.9×10^7	96
29 ^c	3.1×10^7	152
THF ^c	1.0×10^9	4.7
dioxane ^c	8.5×10^8	5.5

^aAt 25 °C; [pyridine] = 0.12 mM except for TMA, where it is 2.4 mmol. Solvent/pentane = 1:1. ^bRate constant from ref 37. ^cRate constant from ref 56. ^d2,3,5,6-tetramethylanisole, ref 59.

negative activation energies, and the concomitant entropic control of reactivity in carbene–alkene additions can “arise in fast reactions having no inherent potential energy barrier”.⁶² The analogous kinetics observed in the reactions of CCl₂ with either trimethoxybenzene or tetramethylethylene is profoundly satisfying.

The complexation of CCl₂ also affects its reactivity. Table 3 records LFP rate constants for the addition of CCl₂ to tetramethylethylene (TME), eq 15, in the presence of various complexing agents. Platz's pyridine ylide methodology was used to determine the rate constants.⁶³



Substitutions of electron-releasing methyl or methoxy groups on the complexing agents additively decelerate the addition of CCl₂ to TME. The three methyl groups of mesitylene (**33**) decrease k_{add} by a factor of 15, while the single methoxy group of anisole (**27**) affords an 18-fold deceleration. Adding four methyl groups to anisole, as in 2,3,5,6-tetramethylanisole (see Figure 6), slows CCl₂ addition by a factor of 96, and three methoxy groups, as in **29**, achieves a 152-fold decrease in k_{add} . On the other hand, simple ethers like THF or dioxane exert limited effects on CCl₂ addition to TME, although they do modulate the additions of halocarbene amides.⁶⁴

Similar reactivity effects upon complexation by aryl ethers have been observed with methylchlorocarbene, benzylchlorocarbene, and *p*-nitrophenylchlorocarbene.⁶⁵ The deceleration of addition could be due to sequestration of the carbene by unproductive, reversibly formed complexes, or it could reflect the kinetics advantage of an uncomplexed and unencumbered carbene, relative to a solvated or complexed species.

Kinetics of Dihalocarbene–Alkene Additions

The dihalocarbenes CCl₂ and CBr₂ were central to early studies of carbenic reactivity.^{48,49} These investigations featured product-based determinations of the relative rates of the carbenes' additions to alkenes, leading to their classification as “electrophiles” (see, however, above).^{48,49,66} The convenient measurement of *absolute* rate constants for additions of the dihalocarbenes to alkenes had to await the introduction of both fast kinetics methodology (LFP), as well as the development of practical syntheses of spectroscopy-friendly carbene precursors. LFP was first applied to halocarbene addition reactions in 1980,⁶⁷ but convenient preparations of dihalodiazirines became available only recently.^{29,30,34a,36,37}

TABLE 4. Absolute Rate Constants (M⁻¹ s⁻¹) for Dihalocarbene Additions^a

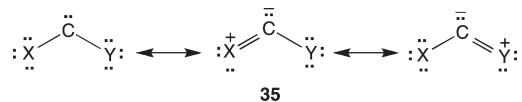
alkene	CCl ₂ ^{b,c}	CClF ^c	CF ₂ ^d
Me ₂ C=CMe ₂	4.7×10^9	1.2×10^9	6.4×10^8
Me ₂ C=CHMe	2.5×10^9	3.8×10^8	1.3×10^8
cyclohexene	6.4×10^7	2.7×10^7	1.4×10^7
<i>n</i> -C ₄ H ₉ CH=CH ₂	1.8×10^7	1.1×10^7	2.4×10^6

^aFrom diazirine photolysis in pentane at 24 °C. Precision in the rate constants is ≤10%; correlation coefficients are ≥0.998. ^bReferences 30 and 37. ^cReference 37. ^dReference 36.

Applying LFP methodology and pyridine ylide visualization to photolyses of DCD, DFD, and chlorofluorodiazirine in various alkenes, we measured absolute rate constants for the additions of CCl₂, CF₂, and CClF to four alkenes, cf. Table 4.^{30,36,37} Two trends, anticipated from earlier relative rate studies, are manifested in Table 4. (1) The carbenes are each electrophilic toward the alkenes; k_{add} increases with increasing alkyl substitution going from the monoalkylated 1-hexene to the tetraalkylated TME.

(2) Toward a given alkene, CX₂ reactivity decreases in the order CCl₂ > CClF > CF₂, the *inverse* of the carbenes' stability ordering (see below). Perhaps surprisingly, CF₂ is only modestly less reactive than CCl₂: k_{add} for CCl₂ exceeds k_{add} for CF₂ only by factors of 5–19 for the alkenes in Table 4. Note that even the absolute rate constants for CBr₂ additions to these alkenes are roughly comparable to those of CCl₂ and less than 100 times greater than those of CF₂.⁶⁸

The classical analysis of dihalocarbene stabilization focuses on resonance donation of halogen lone pairs to the vacant carbenic p orbital, as represented by resonance hybrid **35**. Here, F is more effective than Cl in resonance donation because the 2p–2p overlap of F–C is superior to the 3p–2p overlap of Cl–C. This is reflected in the resonance substituent constants (σ_{R}^+) for F and Cl, which are –0.57 and –0.36, respectively.⁶⁹ Thus, the stability order of our three carbenes should be CF₂ > CClF > CCl₂, whereas the reactivity order, as we observe, is the opposite.



Resonance hybrid **35**, however, represents only the ground states of the dihalocarbenes. A more holistic analysis of their reactivity must also consider the transition states of their addition reactions. In terms of frontier molecular orbital theory, the activation energy for carbene–alkene addition is inversely related to the differential energies of interaction of the carbene and alkene HOMO's and LUMO's; cf. Figure 9.^{44,50,51} For the additions to electron-rich alkenes, like those of Table 4, the alkene-HOMO/carbene-LUMO (p–π) orbital interaction dominates the addition reaction transition state.^{44,50,51} This interaction becomes *less* stabilizing as [$\epsilon^{\text{LU}}(\text{CXY}) - \epsilon^{\text{HO}}(\text{alkene})$] *increases*, where ϵ represents orbital energy. For a given alkene, this means that E_{a} will increase, and k_{add} will decrease, as $\epsilon^{\text{LU}}(\text{CXY})$ increases. The 4-31G computed CXY LUMO energies (in eV) decrease in the order CF₂ (1.89) > CClF (1.03) > CCl₂ (0.31), so that k_{add} should increase in the order CF₂ < CClF < CCl₂, as we observe.

Due to its strongly donating methoxy substituent ($\sigma_{\text{R}}^+ = -1.02$), the LUMO energy of methoxychlorocarbene

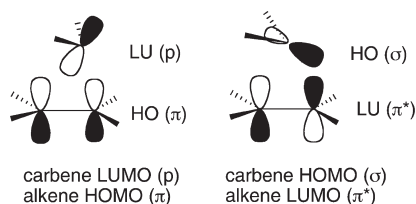


FIGURE 9. Frontier molecular orbital interactions in carbene/alkene additions. Reprinted with permission from ref 2.

(MeOCCl) is significantly higher than that of CF_2 , viz. 2.46 eV versus 1.89 eV. Accordingly, we would expect MeOCCl to be much less reactive than CF_2 toward, e.g., TME. This is indeed observed: $k_{\text{add}} = 4.9 \times 10^3 \text{ M}^{-1} \text{ s}^{-1}$ for MeOCCl⁷⁰ versus $6.4 \times 10^8 \text{ M}^{-1} \text{ s}^{-1}$ for CF_2 , a reactivity decrease of 1.3×10^5 .

Activation Parameters for Dihalocarbene Additions

Until very recently, activation energies and entropies had not been measured for the additions of dihalocarbenes to alkenes, mainly due to the absence of appropriate precursors for the requisite kinetics experiments. Now that diazirine precursors for CCl_2 , CClF , and CF_2 are in hand, we can address these lacunae.

Activation parameters for arylhalocarbenes include very low or even negative activation energies. For example, $E_a = -1.7 \text{ kcal/mol}$ for the addition of PhCCl to TME in the temperature range $263 < T < 300 \text{ K}$.^{61,71} For such an exothermic reaction, Houk suggested that enthalpy continually decreases along the reaction coordinate so that $\Delta H^\ddagger < 0$. The PhCCl –TME reaction possesses a free energy barrier ($\Delta G^\ddagger > 0$) only because of its very negative entropy of activation, $\Delta S^\ddagger = -28 \text{ eu}$.^{62,71}

What is the situation for the dihalocarbenes? There was much discussion in the literature through 1989,^{61,62,71–74} but interest waned in the absence of new data. To characterize the prevailing consensus,⁷⁵ CCl_2 additions were predicted to be dominated by entropic factors, but additions of CF_2 were expected to be controlled by enthalpy.

Our experimental results are nicely illustrated by the additions of CCl_2 , CClF , and CF_2 to TME. Arrhenius correlations of $\ln k_{\text{add}}$ versus $1/T$ for the CCl_2 and CF_2 additions appear in Figures 10 and 11, respectively.^{36,53} Just as the addition of PhCCl affords a curved Arrhenius correlation, the analogous correlation for CCl_2 also curves at higher temperatures. Below 30°C , however, the correlation is linear (Figure 10) and exhibits a *negative* activation energy, $E_a = -1.2 \text{ kcal/mol}$. In contrast, the addition of CF_2 to TME affords a normal, linear Arrhenius correlation, with $E_a = 3.0 \text{ kcal/mol}$ (Figure 11). The E_a for CClF /TME is also “normal” with an intermediate, slightly positive value of 0.9 kcal/mol .

Recalling that the stability order of these three carbenes is $\text{CF}_2 > \text{CClF} > \text{CCl}_2$, we see that E_a (and therefore ΔH^\ddagger) increases with increasing carbenic stability.⁷⁶ With the less reactive alkene, cyclohexene, all three carbenes give normal Arrhenius correlations, shifted to higher activation energies but retaining the same order: CF_2 (7.1 kcal/mol) $>$ CClF (5.9 kcal/mol) $>$ CCl_2 (3.6 kcal/mol).^{36,53}

Table 5 summarizes the activation parameters for the additions of CF_2 , CClF , and CCl_2 to TME, cyclohexene,

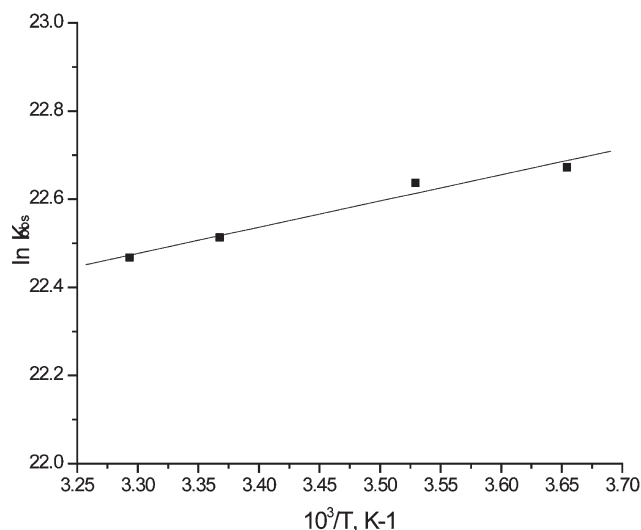


FIGURE 10. Arrhenius correlation for the addition of CCl_2 to TME: $\ln k_{\text{add}}$ vs $1/T$ (273–304 K); $E_a = -1.2 \text{ kcal/mol}$; $r = 0.985$.

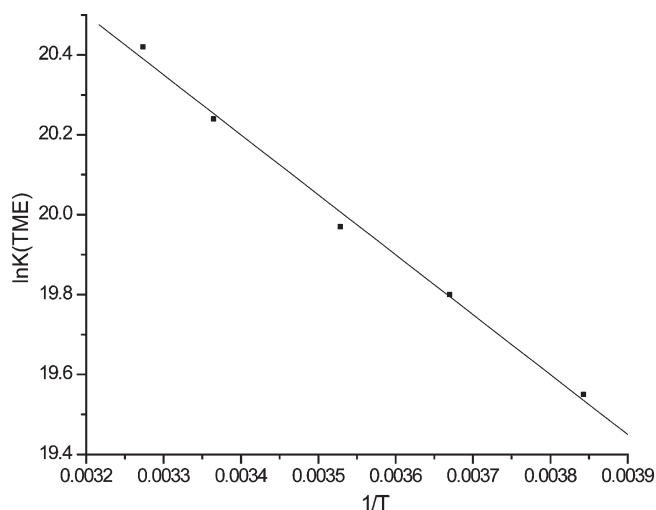


FIGURE 11. Arrhenius correlation for the addition of CF_2 to TME: $\ln k_{\text{add}}$ vs $1/T$; $E_a = 3.0 \text{ kcal/mol}$; $r = -0.997$.

and 1-hexene.^{2,36,53} Several anticipated reactivity trends are evident in Table 5. (1) For each carbene, E_a (and ΔH^\ddagger) increase in the order of increasing carbenic stability, which can be described in terms of substituent resonance donation, carbene stabilization energy, or dihalocarbene orbital energies.^{44,51} (2) For each carbene, E_a decreases as the alkene becomes more reactive, i.e., as the number of alkyl substituents (and electron richness) increases. The E_a ordering, 1-hexene $>$ cyclohexene $>$ TME, is consistent with electrophilic behavior of the dihalocarbenes toward these alkenes and indicative of a dominant carbene-LUMO/alkene-HOMO transition state interaction (cf. Figure 9). (3) Additions of CCl_2 and CClF to the very reactive TME are entropy-controlled ($-T\Delta S^\ddagger > \Delta H^\ddagger$), whereas these parameters are nearly equal for CF_2 . With the less reactive alkenes, cyclohexene and 1-hexene, $\Delta H^\ddagger > -T\Delta S^\ddagger$, and ΔG^\ddagger is dominated by its enthalpic component with all three carbenes.

An unexpected and puzzling trend is the observed decrease of $-T\Delta S^\ddagger$ in parallel to the increase of E_a or ΔH^\ddagger . The net

TABLE 5. Activation Parameters for Dihalocarbene Additions^a

carbene	alkene ^b	E_a	$\log A$	ΔH^\ddagger	ΔS^\ddagger	$-T\Delta S^\ddagger$	ΔG^\ddagger
$\text{CCl}_2^{c,d}$	TME	-1.2 (0.02)	8.8	-1.8	-20 (0.2)	6.0	4.2 (0.2)
CClF^e	TME	0.9 (0.02)	9.7	0.3	-16 (0.2)	4.7	5.0 (0.2)
CF_2^e	TME	3.0 (0.05)	11.0	2.5	-10 (0.3)	3.0	5.5 (0.3)
CCl_2^c	<i>c</i> - C_6H_{10}	3.8 (0.02)	10.9	3.3	-10.5 (1.3)	3.1	6.4 (0.4)
CClF^e	<i>c</i> - C_6H_{10}	5.6 (0.3)	11.5	5.0	-7.8 (1.1)	2.3	7.3 (0.4)
CF_2^e	<i>c</i> - C_6H_{10}	6.9 (0.2)	12.3	6.3	-4.3 (0.5)	1.3	7.6 (0.5)
CCl_2^c	1-hexene	4.7 (0.02)	10.7	4.1	-11.5 (1.1)	3.4	7.3 (0.4)
CClF^e	1-hexene	5.6 (0.3)	11.5	5.4	-7.8 (0.2)	2.3	7.7 (0.3)
CF_2^f	1-hexene	8.0 (0.07)	12.4	7.4	-3.9 (0.2)	1.1	8.6 (0.1)

^aUnits are kcal/mol for E_a , ΔH^\ddagger , $-T\Delta S^\ddagger$, and ΔG^\ddagger ; $\text{M}^{-1}\text{s}^{-1}$ for $\log A$; cal(deg mol) for ΔS^\ddagger . ΔH^\ddagger is calculated at 283 K; ΔG^\ddagger is calculated at 298 K. Errors (in parentheses) are shown for key parameters and are average deviations of two independent determinations. ^bTME = tetramethylethylene; *c*- C_6H_{10} = cyclohexene. ^cFrom ref 53. ^dThe negative activation energy for CCl_2 refers to $273 < T < 304$ K. ^eFrom ref 36. ^fWang, L. Unpublished work; cf. ref 2. Table reprinted with permission from ref 2.

TABLE 6. Activation Parameters for Carbene Additions to TME^a

carbene	E_a	ΔH^\ddagger	ΔS^\ddagger	$-T\Delta S^\ddagger$	ΔG^\ddagger
CCl_2^b	-1.2	-1.8	-20	6.0	4.2
CClF^b	0.9	0.3	-16	4.7	5.0
CF_2^b	3.0	2.5	-10	3.0	5.5
MeOCCl^c	5.8	5.2	-24	7.2	12.4

^aTetramethylethylene. ^bFrom ref 36. ^cFrom ref 70.

effect of this “compensation” is to decrease the contribution of $-T\Delta S^\ddagger$ to ΔG^\ddagger as the contribution of ΔH^\ddagger increases. Consequently, ΔG^\ddagger increases (and k_{add} decreases) only in small steps as CCl_2 changes to CClF and then to CF_2 . Normally, one expects ΔS^\ddagger to become more negative as the carbene becomes more stable and the transition state of its addition reaction becomes later and tighter.^{62,71,73} The ΔS^\ddagger data in Table 5, however, display the opposite, counter-intuitive order, a situation that is not rationalized by DFT calculations which furnish ΔS^\ddagger values that are considerably more negative than the experimental data. Perhaps a resolution can be found in a consideration of dynamic effects in these reactions, and studies of reaction trajectories instead of (or in addition to) classical transition state theory and potential energy surface calculations.

Interestingly, $\Delta H^\ddagger/\Delta S^\ddagger$ compensation is not exhibited by MeOCCl . Activation parameters for its addition to TME appear in Table 6, together with corresponding data for the dihalocarbenes. In terms of carbene stabilization energies, MeOCCl (60.3 kcal/mol) and CF_2 (62.8 kcal/mol) are comparable, yet MeOCCl is much less reactive than CF_2 toward TME. E_a and ΔH^\ddagger are ~ 2 times greater for the MeOCCl addition,⁷⁷ and in keeping with classical ideas, ΔS^\ddagger is much more negative for this reaction than for the corresponding CF_2 addition. Of course, there is a possible steric problem between the “large” MeO carbene substituent and the tetra-substituted olefin.

Other (anticipated) trends apparent in Table 6 include: (1) E_a 's increase in the order of increasing carbene LUMO energies $\text{CCl}_2 < \text{CClF} < \text{CF}_2 < \text{MeOCCl}$.⁷⁸ (2) MeOCCl exhibits the highest E_a yet measured for a carbene addition to TME. (3) Despite the high E_a , the addition of MeOCCl to TME is entropy-controlled; $-T\Delta S^\ddagger > \Delta H^\ddagger$.

Conclusion

A combination of the Graham oxidation of amidines and the diazirine exchange reaction opened synthetic pathways to dihalodiazirine precursors of CCl_2 , CF_2 , and CClF . Using

laser flash photolysis, we examined the formation of trihalomethide carbanions, focusing on the chemistry of bromodichloromethide, CCl_2Br^- . A detailed study of the alkene additions of CCl_2 revealed its inherent ambiphilicity and its nucleophilic behavior toward a sufficiently electron-deficient alkene. Laser flash photolysis with UV-vis detection demonstrated complex formation between CCl_2 and a variety of aromatic ethers. These complexes modulated the rate of CCl_2 addition to tetramethylethylene. Finally, absolute kinetics and activation barriers were measured for the additions of CCl_2 , CF_2 , and CClF to several alkenes and the observed structure–reactivity trends were analyzed.

Acknowledgment. The recent experimental work described here was performed by a very talented group of postdoctoral associates: Drs. Gaosheng Chu, Jingzhi Tian, Lei Wang, and Min Zhang. The computational studies were carried out by my Rutgers colleagues, Professors Karsten Krogh-Jespersen and Ronald R. Sauers. I am much beholden to all of my collaborators. We are grateful to the National Science Foundation and the Petroleum Research Fund for financial support.

References

- (1) Presented in part at the Arthur C. Cope Award Symposium at the 240th American Chemical Society National Meeting in Boston, MA, August 24, 2010.
- (2) This perspective article incorporates some material previously reviewed in: Moss, R. A. *J. Phys. Org. Chem.* **2010**, *23*, 293.
- (3) Hine, J. *J. Am. Chem. Soc.* **1950**, *72*, 2438.
- (4) In his early papers, Hine used “carbon dichloride” and “dichloromethylene” to refer to CCl_2 . The carbene nomenclature was originated by W. v. E. Doering, S. Weinstein, and R. B. Woodward “in a nocturnal Chicago taxi and later delivered diurnally” at the 1951 Boston ACS meeting; cf. Doering, W.v.E.; Knox, L. H. *J. Am. Chem. Soc.* **1956**, *78*, 4947, ref 9.
- (5) Geuther, A. *Ann.* **1862**, *123*, 121.
- (6) Nef, J. U. *Ann.* **1897**, *298*, 367.
- (7) Thiele, J.; Dent, F. *Ann.* **1898**, *302*, 273.
- (8) Mossler, G. *Monatsheft* **1903**, *29*, 573.
- (9) Hine, J. *Divalent Carbon*; Ronald Press: New York, 1964; p 36f.
- (10) Hine, J.; Dowell, A. M., Jr. *J. Am. Chem. Soc.* **1954**, *76*, 2688.
- (11) (a) Hine, J.; Burske, N. W.; Hine, M.; Langford, P. B. *J. Am. Chem. Soc.* **1957**, *79*, 1406. (b) Hine, J.; Ehrenson, S. J. *J. Am. Chem. Soc.* **1958**, *80*, 824. (c) Hine, J.; Prosser, F. P. *J. Am. Chem. Soc.* **1958**, *80*, 4282.
- (12) (a) Hine, J.; Langford, P. B. *J. Am. Chem. Soc.* **1957**, *79*, 5497. (b) Hine, J.; Ketley, A. D. *J. Org. Chem.* **1960**, *25*, 606.
- (13) Doering, W.v.E.; Hoffmann, A. K. *J. Am. Chem. Soc.* **1954**, *76*, 6162.
- (14) For a recent review, see: Fedorynski, M. *Chem. Rev.* **2003**, *103*, 1099.
- (15) Dehmlow, E. V. In *Carbene (Carbenoide) Methoden der Organischen Chemie (Houben-Weyl)*; Regitz, M., Ed.; Thieme Verlag: Stuttgart, 1989; Vol. E19b, pp 1521–1589.
- (16) (a) Makosza, M.; Wawrzyniewicz *Tetrahedron Lett.* **1969**, *10*, 4659. (b) Makosza, M. *Pure Appl. Chem.* **1975**, *43*, 439.

- (17) (a) Wagner, W. M. *Proc. Chem. Soc.* **1959**, 229. (b) Wagner, W. M.; Kloosterziel, H.; Van der Ven, S. *Rec. Trav. Chim. Pays-Bas* **1961**, 80, 740.
- (18) Parham, W. E.; Schweizer, E. E. *J. Org. Chem.* **1959**, 24, 1733.
- (19) (a) Seyferth, D. *Acc. Chem. Res.* **1972**, 5, 65. (b) Seyferth, D.; Burlitch, J. M.; Minas, R. J.; Mui, J.Y.-P.; Simmons, H. D., Jr.; Treiber, A. J. H.; Dowd, S. R. *J. Am. Chem. Soc.* **1965**, 87, 4259.
- (20) Köbrich, G.; Büttner, H.; Wagner, E. *Angew. Chem., Int. Ed. Engl.* **1970**, 9, 169.
- (21) Jones, M., Jr.; Sachs, W. H.; Kulczycki, A.; Waller, F. J. *J. Am. Chem. Soc.* **1966**, 88, 3167.
- (22) Hartwig, J. F.; Jones, M., Jr.; Moss, R. A.; Lawrynowicz, W. *Tetrahedron Lett.* **1986**, 27, 5907.
- (23) Chateuneuf, J. E.; Johnson, R. P.; Kirchoff, M. M. *J. Am. Chem. Soc.* **1990**, 112, 3217.
- (24) Presolski, S. I.; Zorba, A.; Thamattor, D. M.; Tippmann, E. M.; Platz, M. S. *Tetrahedron Lett.* **2004**, 45, 485.
- (25) Graham, W. H. *J. Am. Chem. Soc.* **1965**, 87, 4396.
- (26) Moss, R. A. *Acc. Chem. Res.* **2006**, 39, 267.
- (27) See ref 26 for essential references and a detailed discussion.
- (28) Wlostowska, J.; Moss, R. A.; Guo, W.; Chang, M. J. *Chem. Commun.* **1982**, 432.
- (29) Chu, G.; Moss, R. A.; Sauers, R. R. *J. Am. Chem. Soc.* **2005**, 127, 14206.
- (30) Moss, R. A.; Tian, J.; Sauers, R. R.; Ess, D. H.; Houk, K. N.; Krogh-Jespersen, K. *J. Am. Chem. Soc.* **2007**, 129, 5167.
- (31) Fedé, J.-M.; Jockusch, S.; Lin, N.; Moss, R. A.; Turro, N. J. *Org. Lett.* **2003**, 5, 5027.
- (32) Moss, R. A.; Perez, L. A.; Wlostowska, J.; Guo, W.; Krogh-Jespersen, K. *J. Org. Chem.* **1982**, 47, 4177.
- (33) In our initial preparation of dichlorodiazirine, we used *p*-nitrophenoxychlorodiazirine instead of the 2,4-dinitrophenox derivative **9**. The latter, however, proved to be a more reactive and better substrate.
- (34) (a) Moss, R. A.; Chu, G.; Sauers, R. R. *J. Am. Chem. Soc.* **2005**, 127, 2408. (b) Korkin, A. A.; Schleyer, P.v.R.; Boyd, R. J. *Chem. Phys. Lett.* **1994**, 227, 312.
- (35) Shaffer, C. J.; Esselman, B. J.; McMahon, R. J.; Stanton, J. F.; Woods, R. C. *J. Org. Chem.* **2010**, 75, 1815.
- (36) Moss, R. A.; Wang, L.; Krogh-Jespersen, K. *J. Am. Chem. Soc.* **2009**, 131, 2128.
- (37) Moss, R. A.; Tian, J.; Sauers, R. R.; Skalit, C.; Krogh-Jespersen, K. *Org. Lett.* **2007**, 9, 4053.
- (38) (a) Cox, D. P.; Moss, R. A.; Terpinski, J. *J. Am. Chem. Soc.* **1983**, 105, 6513. (b) Moss, R. A.; Terpinski, J.; Cox, D. P.; Denney, D. Z.; Krogh-Jespersen, K. *J. Am. Chem. Soc.* **1985**, 107, 2743.
- (39) (a) Mitsch, R. A. *J. Heterocycl. Chem.* **1966**, 3, 245. (b) Mitsch, R. A. *J. Heterocycl. Chem.* **1964**, 1, 59. (c) Mitsch, R. A. *J. Org. Chem.* **1968**, 33, 1847.
- (40) Zollinger, J. L.; Wright, C. D.; McBrady, J. J.; Dybvig, D. H.; Fleming, F. A.; Kurhajec, G. A.; Mitsch, R. A.; Neuvar, E. W. *J. Org. Chem.* **1973**, 38, 1065.
- (41) Meyers, M. D.; Frank, S. *Inorg. Chem.* **1966**, 5, 1455.
- (42) Mitsch, R. A.; Neuvar, E. W.; Koshar, R. J.; Dybvig, D. H. *J. Heterocycl. Chem.* **1965**, 2, 371.
- (43) Moss, R. A.; Zhang, M.; Krogh-Jespersen, K. *Org. Lett.* **2009**, 11, 5702.
- (44) Moss, R. A. *Acc. Chem. Res.* **1980**, 13, 58.
- (45) Moss, R. A.; Zhang, M.; Krogh-Jespersen, K. *Org. Lett.* **2009**, 11, 1947.
- (46) (a) Moss, R. A.; Tian, J. *J. Am. Chem. Soc.* **2005**, 127, 8960. (b) Moss, R. A.; Tian, J. *Org. Lett.* **2006**, 8, 1245. (c) Moss, R. A.; Tian, J. *Tetrahedron Lett.* **2006**, 47, 3419.
- (47) The loss of Br⁻ from CCl₂Br⁻ should be considerably faster than the loss of Cl⁻.
- (48) Doering, W.v.E.; Henderson, W. A., Jr. *J. Am. Chem. Soc.* **1958**, 80, 5274.
- (49) Skell, P. S.; Garner, A. Y. *J. Am. Chem. Soc.* **1956**, 78, 5430.
- (50) Moss, R. A. *Acc. Chem. Res.* **1989**, 22, 15.
- (51) Rondan, N. G.; Houk, K. N.; Moss, R. A. *J. Am. Chem. Soc.* **1980**, 102, 1770.
- (52) For a recent review, see: Moss, R. A. In *Carbene Chemistry: From Fleeting Intermediates to Powerful Reagents*; Bertrand, G., Ed.; Dekker: New York, 2002; p 57f.
- (53) Moss, R. A.; Wang, L.; Zhang, M.; Skalit, C.; Krogh-Jespersen, K. *J. Am. Chem. Soc.* **2008**, 130, 5634.
- (54) Moss, R. A.; Tian, J.; Sauers, R. R.; Krogh-Jespersen, K. *J. Am. Chem. Soc.* **2007**, 129, 10019.
- (55) Krogh-Jespersen, K.; Yan, S.; Moss, R. A. *J. Am. Chem. Soc.* **1999**, 121, 6269.
- (56) Moss, R. A.; Wang, L.; Odorisio, C. M.; Zhang, M.; Krogh-Jespersen, K. *J. Phys. Chem. A* **2010**, 114, 209.
- (57) These LFP experiments were performed under nitrogen to prevent the formation of the CCl₂ carbonyl oxide which absorbs at 465 nm.
- (58) The origin of this barrier is discussed below.
- (59) Moss, R. A.; Wang, L.; Odorisio, C. M.; Krogh-Jespersen, K. *Tetrahedron Lett.* **2010**, 51, 1467.
- (60) The C(3) π -complex should absorb at 511 nm ($f \sim 0.1$) and most likely correlates with the observed absorbance at 532 nm. A computed *O*-ylidic complex, absorbing at 464 nm, is not observed.
- (61) Turro, N. J.; Lehr, G. F.; Butcher, J. A., Jr.; Moss, R. A.; Guo, W. *J. Am. Chem. Soc.* **1982**, 104, 1754.
- (62) (a) Houk, K. N.; Rondan, N. G. *J. Am. Chem. Soc.* **1984**, 106, 4293. (b) Houk, K. N.; Rondan, N. G.; Mareda, J. *Tetrahedron* **1985**, 41, 1555.
- (63) Jackson, J. E.; Soundararajan, N.; Platz, M. S.; Liu, M. T. H. *J. Am. Chem. Soc.* **1988**, 110, 5595.
- (64) Tippmann, E. M.; Platz, M. S.; Svir, I. B.; Klymenko, O. *J. Am. Chem. Soc.* **2004**, 126, 5750.
- (65) Moss, R. A.; Wang, L.; Weintraub, E.; Krogh-Jespersen, K. *J. Phys. Chem. A* **2008**, 112, 4651.
- (66) For a review, see: Moss, R. A. In *Carbenes*; Jones, M., Jr., Moss, R. A., Eds.; Wiley: New York, 1973; p 153f.
- (67) For phenylchlorocarbene additions, see: Turro, N. J.; Butcher, J. A.; Moss, R. A.; Guo, W.; Munjal, R. C.; Fedorynski, M. *J. Am. Chem. Soc.* **1980**, 102, 7576.
- (68) Robert, M.; Snoonian, J. R.; Platz, M. S.; Wu, G.; Hong, H.; Thamattoor, D. M.; Jones, M., Jr. *J. Phys. Chem. A* **1988**, 102, 587.
- (69) Ehrenson, R. T. C.; Brownlee, R. W.; Taft, R. W. *Prog. Phys. Org. Chem.* **1973**, 10, 1.
- (70) Moss, R. A.; Zhang, M. *Org. Lett.* **2008**, 10, 4045.
- (71) Moss, R. A.; Lawrynowicz, W.; Turro, N. J.; Gould, I. R.; Cha, Y. *J. Am. Chem. Soc.* **1986**, 108, 7028.
- (72) Gould, I. R.; Turro, N. J.; Butcher, J. A., Jr.; Doublday, C. E., Jr.; Hacker, N. P.; Lehr, G. F.; Moss, R. A.; Cox, D. P.; Guo, W.; Munjal, R. C.; Perez, L. A.; Fedorynski, M. *Tetrahedron* **1985**, 41, 1587.
- (73) (a) Skell, P. S.; Cholod, M. S. *J. Am. Chem. Soc.* **1969**, 91, 7131. (b) Giese, B.; Meister, J. *Angew. Chem., Int. Ed. Engl.* **1978**, 17, 595. (c) Giese, B.; Lee, W.-B. *Angew. Chem., Int. Ed. Engl.* **1980**, 19, 835. (d) Giese, B.; Lee, W.-B.; Meister, J. *Ann. Chem.* **1980**, 725. (e) Giese, B.; Lee, W.-B. *Chem. Ber.* **1981**, 114, 3306.
- (74) Blake, J. F.; Wierschke, S. G.; Jorgensen, W. L. *J. Am. Chem. Soc.* **1989**, 111, 1919.
- (75) See the summary in ref 53.
- (76) The computed carbene stabilization energies, relative to methylene (CH₂), are in kcal/mol: CF₂ (62.8), CClF (42.8), and CCl₂ (26.5).
- (77) The carbene-LUMO/alkene-HOMO interaction is ~ 0.6 eV less favorable in the MeOCCl/TME addition compared to the CF₂/TME addition.
- (78) Computed carbene LUMO (p orbital energies) in eV are: CCl₂, 0.31; CClF, 1.03; CF₂, 1.89; MeOCCl, 2.46.